



CHORUS

This is the accepted manuscript made available via CHORUS. The article has been published as:

Correlated Electron State in $\text{Ce}_{1-x}\text{Yb}_x\text{CoIn}_5$ Stabilized by Cooperative Valence Fluctuations

L. Shu, R. E. Baumbach, M. Janoschek, E. Gonzales, K. Huang, T. A. Sayles, J. Paglione, J. O'Brien, J. J. Hamlin, D. A. Zocco, P.-C. Ho, C. A. McElroy, and M. B. Maple

Phys. Rev. Lett. **106**, 156403 — Published 13 April 2011

DOI: [10.1103/PhysRevLett.106.156403](https://doi.org/10.1103/PhysRevLett.106.156403)

Correlated Electron State in $\text{Ce}_{1-x}\text{Yb}_x\text{CoIn}_5$ Stabilized by Cooperative Valence Fluctuations

Lei Shu,¹ R. E. Baumbach,¹ M. Janoschek,¹ E. Gonzales,¹ K. Huang,¹ T. A. Sayles,¹ J. Paglione,² J. O' Brien,³ J. J. Hamlin,¹ D. A. Zocco,¹ P.-C. Ho,⁴ C. A. McElroy,¹ and M. B. Maple^{1,*}

¹*Department of Physics, University of California, San Diego, La Jolla, California 92093*

²*Center for Nanophysics and Advanced Materials, Department of Physics, University of Maryland, College Park, Maryland 20742*

³*Quantum Design, San Diego, California 92121*

⁴*Department of Physics, California State University, Fresno, California 93740*

(Dated: February 8, 2011)

X-ray diffraction, electrical resistivity, magnetic susceptibility, and specific heat measurements on the system $\text{Ce}_{1-x}\text{Yb}_x\text{CoIn}_5$ ($0 \leq x \leq 1$) reveal that many of the characteristic features of the $x = 0$ correlated electron state are stable for $0 \leq x \leq 0.775$, and that phase separation occurs for $x > 0.775$. The stability of the correlated electron state is apparently due to cooperative behavior of the Ce and Yb ions, involving their unstable valences. Low temperature Non-Fermi liquid behavior is observed which varies with x , even though there is no readily identifiable quantum critical point. The superconducting critical temperature T_c decreases linearly with x towards 0 K as $x \rightarrow 1$, in contrast to other HF superconductors where T_c scales with T_{coh} .

PACS numbers: 71.10.Hf, 71.27.+a, 74.70.Tx, 75.30.Mb

One of the important issues in the study of correlated electron physics is the relationship between quantum criticality (QC), non-Fermi-liquid (NFL) behavior and unconventional superconductivity (SC). It is generally thought that critical fluctuations associated with a magnetic quantum critical point (QCP), where a second order magnetic phase transition is suppressed to 0 K by an external control parameter (e.g., composition (x), pressure (P), magnetic field (H)), can provide a mechanism for NFL behavior and unconventional SC in a narrow ‘‘dome’’ around the QCP [1] (e.g., CeIn_3 , CePd_2Si_2 , and $\text{CeCu}_{6-x}\text{Au}_x$) [2, 3]. However, the precise nature of the relationship between these phenomena remains to be understood, particularly since many compounds have been reported where the NFL behavior persists over an extended region of the phase diagram in the absence of any identifiable QCP [4].

Ce-based compounds have been studied extensively within the context of the QCP scenario because the Ce valence (or, alternatively, the Ce $4f$ electron shell occupation number) is sensitive to applied or chemical pressure, which often allows the magnetic ordering temperature to be tuned towards 0 K. One such family of materials are those with the chemical formula $\text{Ce}M\text{In}_5$ ($M = \text{Co}, \text{Rh}, \text{Ir}$). These compounds exhibit a variety of unusual ground states that appear to be strongly influenced by nearness to QCPs or QC regions in the $T - P - x - H$ phase space. Of these, CeCoIn_5 has been the focus of much attention. It is believed to be situated near an antiferromagnetic (AFM) QCP that can be accessed by ‘‘negative’’ pressure [5], as was demonstrated by a combination of studies involving the application of pressure and substitution of Rh for Co [6]. The normal state electrical resistivity shows NFL-like T -linear behavior, in accord with the system being near to a 2D AFM QCP [5]. Upon application of pressure, the SC transition can be suppressed to 0 K, and a FL like quadratic T -dependence of the electrical resistivity is restored, as expected for the prototypical QCP scenario. A second magnetic field induced QCP is observed upon suppression of the SC

state [7, 8]. In addition, the $H - T$ phase diagram is unusual, in that the transition from the normal to the SC phase is first order at high H [9, 10], and there is a second magnetically ordered SC phase that exists only at low T and high H close to the upper critical field H_{c2} [11].

In this letter, we report results for the series $\text{Ce}_{1-x}\text{Yb}_x\text{CoIn}_5$ which demonstrate that Yb substitution constitutes a useful tuning parameter for exploring QC phenomena in CeCoIn_5 . Initially, our study was motivated by the observation that both Cooper pair breaking and Kondo-lattice coherence are uniformly influenced by magnetic and nonmagnetic substituents (R) for $\text{Ce}_{1-x}R_x\text{CoIn}_5$. In contrast, the NFL behavior is strongly dependent on the f -electron configuration of the R ions [12]. In a simple picture, Yb substitution is expected to yield similar results. However, Yb is distinguished from other rare earth and lanthanide elements in several ways. For instance, Yb frequently exhibits a valence (v) instability ($2+ \leq v_{\text{Yb}} \leq 3+$), similar to Ce ($3+ \leq v_{\text{Ce}} \leq 4+$). Another parallel is found in the electron-hole analogy between Ce^{3+} ($4f^1$) and Yb^{3+} ($4f^{13}$). However, Ce and Yb also exhibit several significant differences: e.g., applied pressure causes Yb to become more magnetic and Ce to become less magnetic.

Our study reveals that as Yb is substituted for Ce, many of the exemplary correlated electron effects that are observed for CeCoIn_5 are only weakly affected, in marked contrast with what is seen for other rare earth (R) substitutions in this system. To summarize: (1) The lattice parameters remain nearly constant for $x \leq 0.775$, after which phase separation into Yb rich and deficient phases of $\text{Ce}_{1-x}\text{Yb}_x\text{CoIn}_5$ occurs. (2) The SC transition temperature is weakly suppressed with x and extends to the phase separation region. The extrapolation of the T_c vs. x curve for $x > 0.775$ suggests that in the absence of phase separation, SC would disappear near $x = 1$. This finding is remarkable, as other R substitutions in $\text{Ce}_{1-x}R_x\text{CoIn}_5$ suppress SC at approximately $x = 0.25$

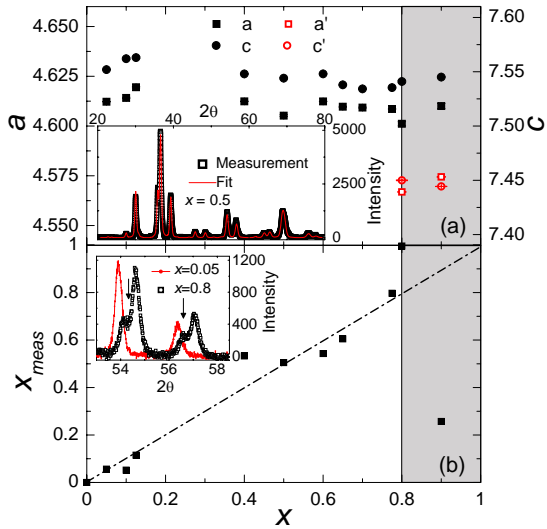


FIG. 1. (a) Lattice parameters a (filled black squares) and c (filled black circles) vs. Yb concentration x for the $\text{Ce}_{1-x}\text{Yb}_x\text{CoIn}_5$ system. Phase separation occurs for $x \geq 0.8$, and two sets of lattice constants are observed, as shown by the red open symbols that correspond to the lattice constants expected for YbCoIn_5 . Inset: Representative X-ray powder diffraction (XRD) profile and Rietveld fit for the $x = 0.5$ sample. (b) Measured Yb concentration x_{meas} from EDX vs. nominal x . Inset: Comparison of the XRD profiles for the $x = 0.05$ and $x = 0.8$ samples, illustrating the phase separation. The arrows highlight the splitting of the Bragg reflections (see text).

[12]. (3) The Kondo-like coherence temperature T_{coh} may be weakly suppressed for low x , after which it remains roughly constant up to $x = 0.775$. These results are particularly striking if we consider that, in contrast to other heavy fermion SCs, T_c does not scale with T_{coh} [13], except possibly for small x . (4) The heavy electron mass and effective magnetic moment remain roughly constant up to $x = 0.775$. (5) The NFL behavior is strongly influenced by Yb substitution and persists

up to $x = 0.65$, after which a recovery of FL-like behavior is observed with increasing x . Taken together, these properties suggest that, unlike in other $\text{Ce}_{1-x}\text{R}_x\text{CoIn}_5$ series, the Ce and Yb ions adopt cooperative intermediate valence (CIV) states, resulting in the preservation of the coherent Kondo-like lattice and SC, while the associated valence fluctuations (VF) strongly tune the NFL state [15].

Single crystals of $\text{Ce}_{1-x}\text{Yb}_x\text{CoIn}_5$ ($0 \leq x \leq 1$) were synthesized using an indium self flux method [14]. The crystal structure and chemical composition were verified by means of X-ray powder diffraction (XRD) and energy dispersive X-ray (EDX) analysis (Fig. 1). The lattice parameters a and c were determined by means of Rietveld refinement (Fig. 1(a)). According to Vegard's law, the lattice constants should decrease linearly with increasing Yb concentration, if there are no changes in the valence of the Ce or Yb ions that would modify their ionic radii, or changes in bonding due to variation in the electron concentration. However, both lattice parameters remain roughly constant as x changes, indicating that the Ce and Yb ions do not retain the valences of the end member compounds ($v_{\text{Ce}} = 3+$ for $x = 0$ and $v_{\text{Yb}} = 2+$ for $x = 1$).

The EDX data reveal that crystals with the expected Yb concentration form for $x < 0.8$. For larger values of x , each peak in the XRD profile splits into two peaks (see inset of Fig. 1(b)), one with low intensity corresponding to the lattice constants for $x < 0.8$ and a second one corresponding to the value expected for pure YbCoIn_5 . The ratio of the integrated intensities for one pair of peaks is ~ 0.49 for the case of $x = 0.8$, indicating phase separation into a minority phase (32%) and a majority phase (68%), that exhibit distinct Yb concentrations, where the latter is the Yb rich phase. The phase separation is further supported by the results of the EDX measurements (shaded region in Fig. 1). Similar results were recently reported by Capan et al. [16].

Electrical resistivity (ρ) measurements were performed using a standard four-wire technique. The shapes of the normalized electrical resistivity $\rho/\rho(300\text{K})$ curves (Fig. 2) for all samples with $x \leq 0.775$ are typical of many HF materials: *i.e.*, the data exhibit a weak T dependence at high T and a maximum or broad hump at T_{coh} that is followed by a decrease in ρ with decreasing T . This behavior is interpreted as the onset of coherent Kondo-like screening of the magnetic sublattice by the conduction electrons at T_{coh} . As the Yb concentration is increased, T_{coh} may be weakly suppressed initially, after which it remains roughly constant (Fig. 5(a)). In contrast, YbCoIn_5 does not exhibit correlated electron effects, suggesting an abrupt change in the behavior of the R sublattice between $0 \leq x \leq 0.775$ and $x = 1$.

The normal-state $\rho(T)$ data between T_c and ~ 25 K for each substitution ($x \leq 0.775$) can be fit with a power law $\rho(T) = \rho_0 + AT^{n_\rho}$ (Fig. 2(b)). A sub- T -linear transport scattering rate (indicative of NFL behavior) is observed [12], which reaches a minimum value of $n_\rho \sim$ near $x = 0.4$, after which it slowly recovers towards $n_\rho \sim 2$ (Fig. 5(c)). For $x = 0.775$, we find that $A \approx 0.036 \mu\Omega\text{cm}/\text{K}^2$, implying that the ground state is a heavy Fermi liquid at this concentration.

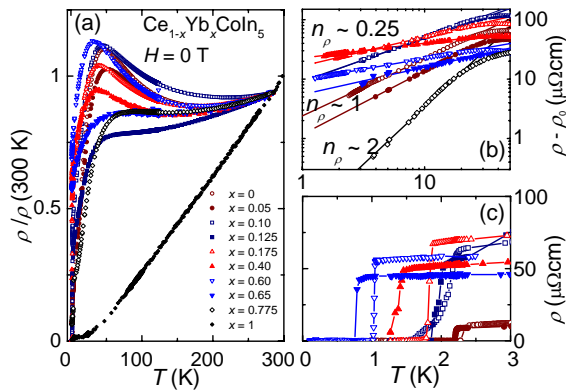


FIG. 2. (a) Electrical resistivity ρ normalized to its value at 300 K, $\rho/\rho(300\text{K})$, vs. temperature T for $\text{Ce}_{1-x}\text{Yb}_x\text{CoIn}_5$ with $0 \leq x \leq 1.0$. (b) Power law fits for the data between T_c and ~ 25 K. (c): Low T resistive superconducting transition curves.

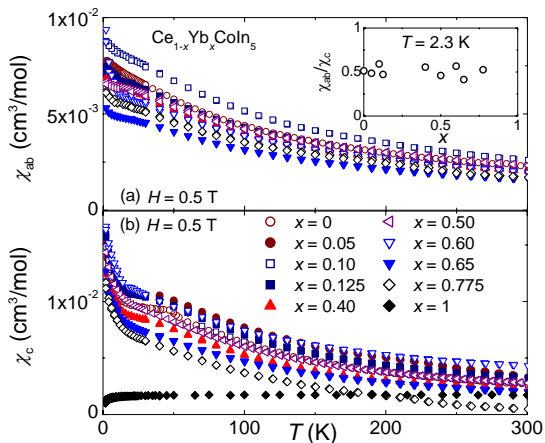


FIG. 3. (a) Magnetic susceptibility along the ab -plane χ_{ab} vs. temperature T for $\text{Ce}_{1-x}\text{Yb}_x\text{CoIn}_5$. Inset: Ratio of χ_{ab} to χ_c at $T = 2.3$ K. (b) Magnetic susceptibility along the c -axis χ_c vs. T for $\text{Ce}_{1-x}\text{Yb}_x\text{CoIn}_5$. Data for $x = 0$ are from Ref. [17].

In order to explore this perspective, we have calculated the Kadowaki-Woods ratio $R_{KW} = A/\gamma^2$, which gives the relationship between the coefficient γ of the electronic specific heat and the coefficient A of the T^2 contribution to the electrical resistivity, assuming that the system exhibits heavy FL behavior at low T . If we consider $\gamma(2.3 \text{ K}) = 140 \text{ mJ/mol-K}^2$ (Table I), then $R_{KW} = 1.86 \times 10^{-6} \mu\Omega\text{cm}(\text{mol-K/mJ})^2$. This value is intermediate between what is expected for Ce- and Yb-based heavy fermion compounds [18, 19], emphasizing that strong electronic correlations persist up to $x \approx 0.775$. SC transitions are clearly observed in $\rho(T)$ for $0 \leq x \leq 0.65$ [Fig. 5(c)], and there is a monotonic suppression of T_c with increasing Yb concentration [Fig. 2(c)]. In particular, we note that the T_c vs. x curve extrapolates to 0 K near $x = 1$, emphasizing that the SC is anomalously robust in the presence of Yb substituents.

Magnetic susceptibility (χ) measurements were carried out as a function of T using a Quantum Design SQUID magnetometer in $H = 0.5$ T. Figures 3(a)-(b) show $\chi(T)$ in the normal state for H applied in the ab -plane, χ_{ab} , and along the c -axis, χ_c . The ratio of χ_{ab} to χ_c at $T = 2.3$ K is ~ 0.5 (inset of Fig. 3(a)). Surprisingly, $\chi(T)$ retains a T -dependence that is nearly identical to that of $x = 0$ for $x \leq 0.775$: i.e., Curie-Weiss behavior is observed at high T , after which $\chi(T)$ saturates below 50 K, consistent with the onset of Kondo-like demagnetization and the coherent behavior observed in $\rho(T)$. These results are contrary to what would be expected if the Yb ions were to enter the lattice in the nonmagnetic divalent state, in which case $\chi(T)$ should scale with $(1-x)$. Finally, $\chi(T)$ again increases upon cooling below 20 K, contrary to the behavior of ideal HF compounds which are expected to remain in a FL state with a nearly T -independent χ as T approaches 0 K. This upturn appears to be an intrinsic effect, and not due to magnetic impurities, since we find that $M(H)$ curves at low T do not saturate up to 70 kOe [20]. Between 1.8 K and ~ 20 K, χ_c can be fit by the form $\chi_c = \chi_c(0) + a/T^{n_x}$, consistent

TABLE I. Superconducting parameters for samples of $\text{Ce}_{1-x}\text{Yb}_x\text{CoIn}_5$. The values of T_c have been determined from specific heat data. ΔC is the jump in $C(T)$ at T_c , $\gamma(2.3 \text{ K})$ is the estimated electronic-specific-heat coefficient at 2.3 K, and n is the power law exponent of $C(T)/T$ below T_c .

x	T_c K	ΔC mJ/mol K	$\gamma(2.3 \text{ K})$ mJ/mol K ²	$\Delta C/\gamma(2.3 \text{ K})T_c$	n
0	2.29	3460	357	4.31	2.2(1)
0.05	2.16	3040	373	3.97	2.5(1)
0.10	2.09	2240	347	2.95	2.7(1)
0.125	1.97	1810	332	2.63	
0.50	1.19	235	330	0.49	1.4(1)
0.65			283		
0.775			140		

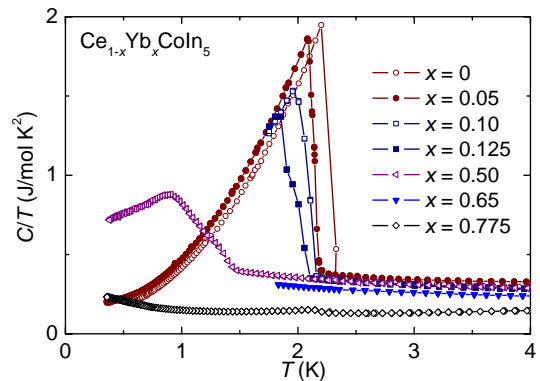


FIG. 4. Specific heat C divided by temperature T vs. T for $\text{Ce}_{1-x}\text{Yb}_x\text{CoIn}_5$.

with the NFL behavior observed in $\rho(T)$ and $C(T)$. Fig. 5(d) shows the parameters n_x .

The specific heat (C) was measured for $0.3 \text{ K} \leq T \leq 5 \text{ K}$ in a Quantum Design Physical Properties Measurement System semiadiabatic calorimeter using a heat-pulse technique. Fig. 4 shows C/T vs. T for several values of x . The electronic specific heat coefficient $\gamma = C/T$, estimated to be the value of C/T near 2.3 K (Table I), reveals a substantial mass renormalization ($\gamma \propto m^*$) that persists up to $x = 0.65$, after which γ is suppressed. Additionally, C/T tends to increase with decreasing T down to the SC transition for all x , indicating that the low T NFL state persists up to $x = 0.775$.

For $x \leq 0.125$, $C(T)/T$ shows abrupt jumps at 2.1-2.3 K, while a broad transition is observed at low T for $x = 0.5$. From these data, we infer bulk SC for all x . To address how the SC state evolves with x , we calculated $\Delta C/\gamma T_c$, which quantifies the strength of the Cooper pair coupling in the BCS model of SC. As shown in Table I, $\Delta C/\gamma T_c$ is gradually suppressed with increasing x . We also studied the T dependence of $C(T)$ below T_c for different values of x . $C(T)$ does not conform to the exponential behavior expected for a conventional BCS SC. Instead, between 0.3 K and 80% of T_c , $C(T)/T$ can be fit by the function $C/T = \gamma_0 + aT^n$, yielding values of n between 1.4 and 2.7 (Table I), suggesting

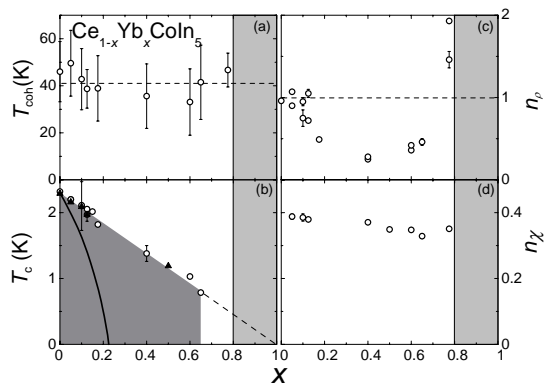


FIG. 5. (a) Coherence temperature T_{coh} , where $\rho(T)$ exhibits a maximum (or knee) vs. x . The error bars represent the width of the maximum, defined as the T $\rho = 0.95\rho_{coh}$. (b) Circles: T_c determined from $\rho(T)$ measurements vs. x for $Ce_{1-x}Yb_xCoIn_5$. The vertical bars correspond to the 90% and 10% values of the superconducting transitions. Triangles: T_c , determined from $C(T)$ measurements vs. x . The solid line shows the suppression of T_c as reported for other rare earth substitutions [12]. (c) Fit parameters n_ρ , extracted from power law $\rho = \rho_0 + AT^{n_\rho}$ fits to the normal state resistivity in zero applied field vs. x (d) Fit parameters n_χ , determined from fits of $\chi_c = \chi_c(0) + a/T^{n_\chi}$ to the normal state $\chi(T)$ vs. x . The light grey shading represents the x range where phase separation is observed.

the occurrence of nodes in SC energy gap. Finally, we note that there is a very small feature in C/T for $x = 0.775$ at $T \sim 2.3$ K, which may be due to a SC transition arising from a CeCoIn₅ impurity phase of 5%, as estimated from the size of the SC jump ΔC . We note, however, that no additional peaks were observed in the XRD profiles for this concentration.

Our measurements demonstrate that $Ce_{1-x}Yb_xCoIn_5$ exhibits an unconventional $T - x$ phase diagram in which there is no apparent QCP, the Kondo-like lattice behavior and SC are preserved up to large values of x , and the NFL state is strongly modified with x (Fig. 5). These observations are striking, since previous studies of other $Ce_{1-x}R_xCoIn_5$ systems have revealed that T_c and T_{coh} are rapidly and uniformly suppressed by both magnetic and nonmagnetic R ions and, from a naive point of view, Yb substitution should yield similar results. Moreover, T_c does not scale with T_{coh} , as would be expected for a typical heavy fermion SC. Thus, it appears that Ce and Yb cooperatively change their electronic states in $Ce_{1-x}Yb_xCoIn_5$ in such a way as to preserve the underlying Kondo-like lattice behavior and SC of CeCoIn₅. In contrast, the NFL state is strongly susceptible to the introduction of Yb ions, as observed for other R substituents in CeCoIn₅.

A possible explanation for this behavior can be found by considering VFs arising from a CIV state formed by the Ce and Yb ions. In this scenario the substituted Yb ions “mimic” the electronic configuration of Ce, resulting in the anomalous preservation of the correlated electron state of the end member compound CeCoIn₅ over a large range of x in $Ce_{1-x}Yb_xCoIn_5$. The CIV state also provides a mechanism that may drive the observed NFL physics. It was recently

suggested that quantum valence criticality yields NFL-like anomalies in the low T specific heat ($C/T \sim -\ln T$), magnetic susceptibility ($\chi \sim T^{-n_\chi}$, $n_\chi = 0.5 - 0.6$) and electrical resistivity ($\Delta\rho \sim T$) as observed in other Yb-based compounds such as β -YbAlB₄ and YbRh₂(Si_{0.95}Ge_{0.05})₂ [15, 21, 22]. We observe a T -linear and sub- T -linear transport scattering rate in ρ , a weak inverse power law in χ , and a low T increase of C/T in the normal state for $Ce_{1-x}Yb_xCoIn_5$. Moreover, QC VFs have been proposed to drive the NFL physics and unconventional SC in CeCu₂(Si_{1-x}Ge_x)₂ [23].

To summarize, the Kondo coherence and SC do not scale with the NFL behavior for $Ce_{1-x}Yb_xCoIn_5$, but ultimately these phenomena may be connected through cooperatively tuned IV states. In this scenario, NFL behavior and unconventional SC coexist over a large part of the phase diagram, in contrast to what is expected for classical QCP systems for which the NFL behavior and unconventional SC are tightly confined to a “V-shaped” region around the QCP. We conclude that $Ce_{1-x}Yb_xCoIn_5$ belongs to a growing class of systems in which the NFL behavior occurs in the absence of an obvious QCP [4]. These results also suggest that VFs may play a role in the unconventional SC and NFL behavior in pure CeCoIn₅.

Crystal growth and characterization were funded by the U.S. DOE under Grants No. DE FG02-04ER46105. Low-temperature measurements were funded by the NSF under Grant No. 0802478. M. J. acknowledges financial support by the Alexander von Humboldt foundation.

* Corresponding Author.
mbmaple@ucsd.edu

- [1] C. M. Varma, Z. Nussinov, and W. v. Saarloos, *Physics Reports* **361**, 267 (2002).
- [2] N. D. Mathur *et al.*, *Nature* **394**, 39 (1998).
- [3] H. v. Löhneysen, *J. Phys. Condens. Matter* **8**, 9689 (1996).
- [4] M. B. Maple *et al.*, *J. Low Temp. Phys.* **161**, 4 (2010).
- [5] V. A. Sidorov *et al.*, *Phys. Rev. Lett.* **89**, 157004 (2002).
- [6] J. R. Jeffries *et al.*, *Phys. Rev. B* **72**, 024551 (2005).
- [7] J. Paglione *et al.*, *Phys. Rev. Lett.* **91**, 246405 (2003).
- [8] A. D. Bianchi *et al.*, *Phys. Rev. Lett.* **91**, 257001 (2003).
- [9] A. D. Bianchi *et al.*, *Phys. Rev. Lett.* **89**, 137002 (2002).
- [10] A. D. Bianchi *et al.*, *Phys. Rev. Lett.* **91**, 187004 (2003).
- [11] H. A. Radovan *et al.*, *Nature* **425**, 51 (2003).
- [12] J. Paglione *et al.*, *Nature Physics* **3**, 703 (2007).
- [13] Y.-F. Yang *et al.*, *Nature* **454**, 611-613 (2008)
- [14] V. S. Zapf *et al.*, *Phys. Rev. B* **65**, 014506 (2001).
- [15] S. Watanabe and K. Miyake, *Phys. Rev. Lett.* **105**, 186403 (2010).
- [16] C. Capan *et al.*, *Europhys. Lett.* **92**, 47004 (2010).
- [17] C. Petrovic *et al.*, *J. Phys.: Condens. Matter* **13**, L337 (2001).
- [18] K. Kadowaki and S. B. Woods, *Solid State Commun.* **58**, 507 (1986).
- [19] N. Tsujii, H. Kontani, and K. Yoshimura, *Phys. Rev. Lett.* **94**, 057201 (2005).
- [20] T. Tayama *et al.*, *Phys. Rev. B* **65**, 180504 (2002).
- [21] J. Custers *et al.*, *Nature* **424**, 524 (2003).
- [22] S. Nakatsuji *et al.*, *Nat. Phys.* **4**, 603 (2008).
- [23] H. Q. Yuan *et al.*, *Phys. Rev. Lett.* **96**, 047008 (2006).